Exploring differential electron transfer kinetics of electrochemical aptamer-based sensors to achieve calibration-free measurements

Man Zhu[§,†], Chongyu Xie[†], Fan Xu[†], Shaoguang Li[†], Hui Li[†,*] Fan Xia[†]

[§]*Faculty of Materials Science and Engineering, Hubei Polytechnic University, Huangshi, Hubei, 435003, Peoples R China.*

[†]*State Key Laboratory of Biogeology and Environmental Geology, Engineering Research Center of Nano-Geomaterials of Ministry of Education, Faculty of Materials Science and Chemistry, China University of Geosciences, Wuhan 430074, China, lihui-chem@cug.edu.cn*

Content

Materials

Adenosine triphosphate (ATP), Kanamycin, 6-Mercapto-1-hexanol, tris(2-carboethyl)-phosphine hydrochloride (TCEP), and tris(hydroxymethyl)aminomethane (Tris) were purchased from Aladdin Co., Ltd. (Shanghai, China). Doxorubicin hydrochloride salt was purchased from Adamas Reagent, Ltd. (Shanghai, China). Bovine serum and blood was purchased from Shanghai Yuanye Bio-Technology Co., Ltd. (Shanghai, China). Thiol-modified DNA aptamer sequences were synthesized by Sangon Biotechnology Co., Ltd. (Shanghai, China), purified by HPLC, confirmed by HPLC profile and mass spectrometry. These were dissolved in 1×PBS buffer (10 mM PB, 137 mM NaCl, and 2.7 mM KCl, pH 7.0) to a final concentration of 100 μM, aliquoted and stored at -20°C prior to use. The sequences used in this study were:

kanamycin aptamer:

5'-HO-$(CH_2)_6$-S-S-$(CH_2)_6$-GGGACTTGGTTTAGGTAATGAGTCCC-MB-3'

ATP aptamer:

5'-HO-$(CH_2)_6$-S-S-$(CH_2)_6$-ACCTGGGGGAGTATTGCGGAGGAAGGT-MB-3'

doxorubicin aptamer:

5'-HO-$(CH_2)_6$-S-S-$(CH_2)_6$-

ACCATCTGTGTAAGGGGTAAGGGGTGGT-MB-3'

Thrombin aptamer:

5'-HO-$(CH_2)_6$-S-S-$(CH_2)_6$-TTTTTTTTTTGGTTGGTGTGGTTGG-MB-3'

Electrode cleaning

The electrodes were cleaned electrochemically by cycling 10 times between 0 and -1.5 V (all potentials versus Ag/AgCl) at 0.1 V s^{-1} in aqueous 0.5 M NaOH using a three electrode setup (the platinum wire electrode as the counter electrode, Ag/AgCl as the reference electrode and gold as the working electrode). Then the gold electrodes were rinsed thoroughly with ultrapure water, transferred into 0.5 M H_2SO_4 and applied a chronoamperometry procedure with $E_{initial}$ = 0.0 V and E_{high} = 2.0 V vs Ag/AgCl for 320 steps and each pulse being of 0.02 s duration. Finally, the gold electrodes were transferred into 0.05 M H_2SO_4 using cyclic voltammetry at 0.1 V s^{-1} between 0 and 1.65 V to observe integrating the area under the curve of the gold oxide reduction peak, which then dividing it by 422 μC/cm^2 to determine the electroactive area of each gold electrode. Freshly cleaned electrodes typically exhibit a surface area of ~0.03 (±30%) cm^2.

Sensor fabrication

The freshly cleaned electrodes were immersed in 1 μM DNA solution

and assembled at room temperature for 2 hours, which was previously prepared by incubating a solution of 100 μM thiolated DNA and 20 mM tris-(2-carboxyethyl) phosphine hydrochloride (TCEP) (1:200) for 1 hour at room temperature, and further diluted by 1×PBS buffer.

Then the resulting sensors were washed with pure water. The functionalized sensors were then rinsed with pure water prior to use.

Electrochemical measurements

Electrochemical measurements were performed at room temperature using a CHI1040C potentiostat and a standard three-electrode cell containing a platinum counter electrode and an Ag/AgCl (3 M KCl) reference electrode.

The pH of tris buffer solution for thrombin detection was 7.4, and the solution contained 140 mM NaCl, 20 mM $MgCl_2$ and 20 mM KCl. For the detection of thrombin in tris buffer (pH 7.4), the thrombin-detecting sensors were pre-swept for two hours to stabilize the sensors before the further tests. Meanwhile, the 50% diluted blood serum was composed of 0.2 M tris buffer mixed with blood serum (1:1).

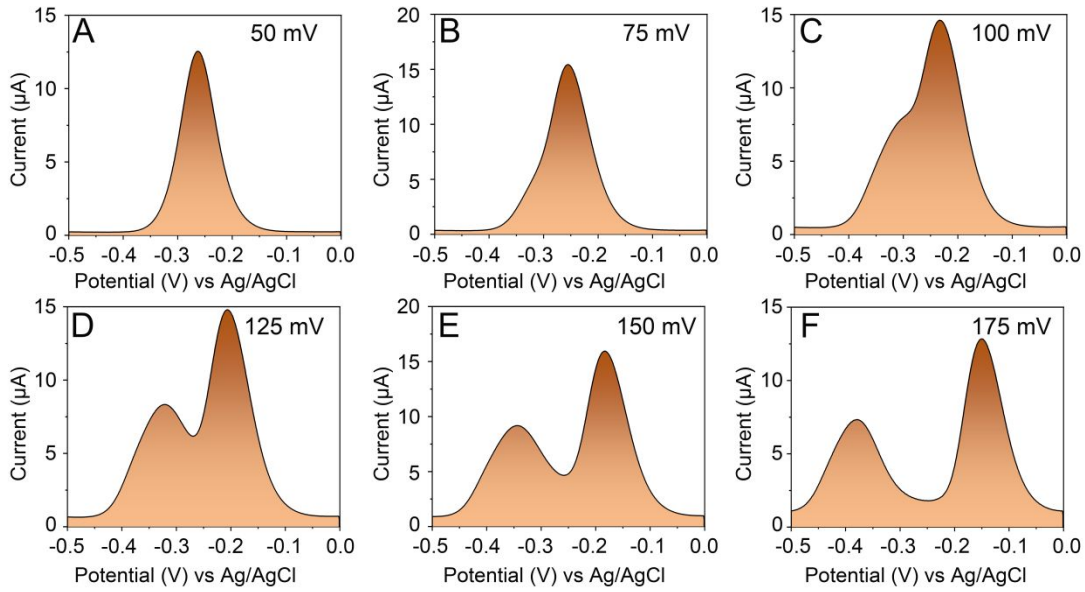

Figure S1. The SWV curves of the kanamycin-detecting sensors were obtained in PBS buffer at frequencies of 60 Hz and amplitude of (A) 50 mV, (B) 75 mV, (C) 100 mV, (D) 125 mV, (E) 150 mV and (F) 175 mV, respectively.

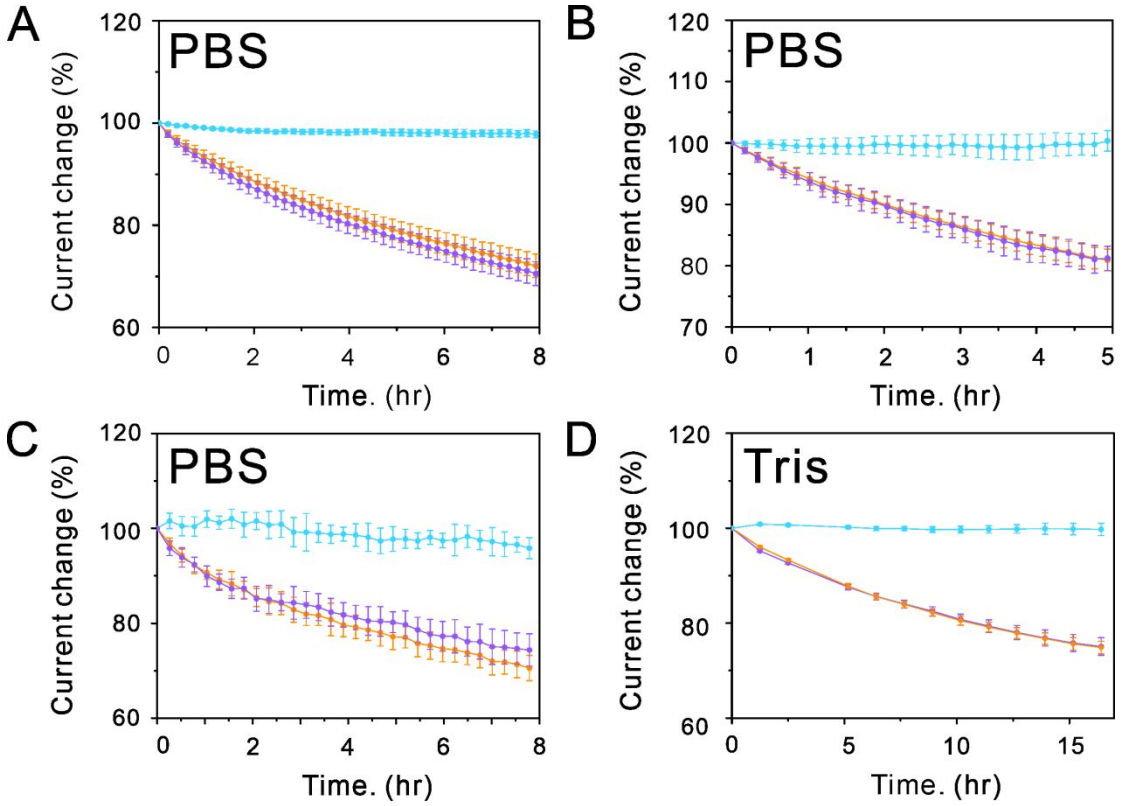

Figure S2. The stability in buffer solution for the sensors with "dual-peak" strategy without calibration (yellow curve: high potential peak; purple curve: low potential peak;

blue curve: the ratio). (A) The kanamycin-detecting sensors test in PBS. (B) The ATP-detecting sensors test in PBS. (C) The doxorubicin-detecting sensors test in PBS. (D) The thrombin-detecting sensors test in tris buffer. All data show that the ratio signal is more stable than the left or right peak.

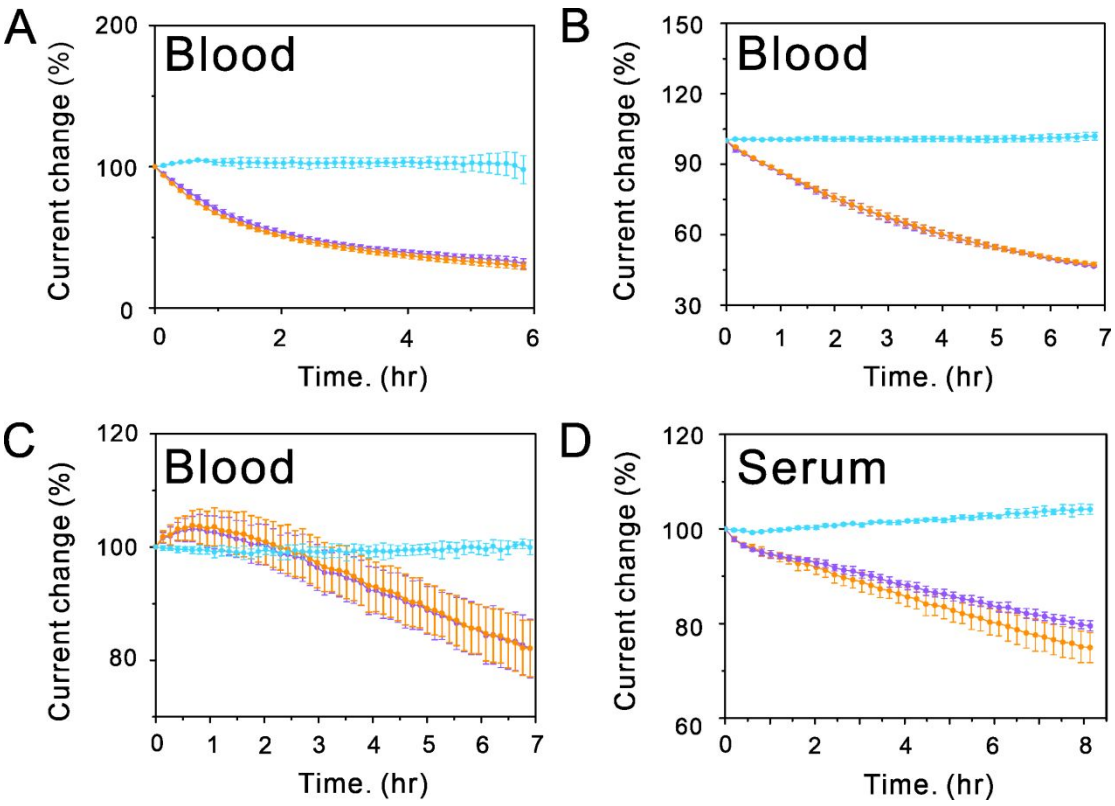

Figure S3. The stability in complex solution for the sensors with "dual-peak" strategy without calibration (yellow curve: high potential peak; purple curve: low potential peak; blue curve: the ratio). (A) The kanamycin-detecting sensors test in whole blood. (B) The ATP-detecting sensors test in whole blood. (C) The doxorubicin-detecting sensors test in whole blood. (D) The thrombin-detecting sensors test in diluted serum. All data show that the ratio signal is more stable than the left or right peak.

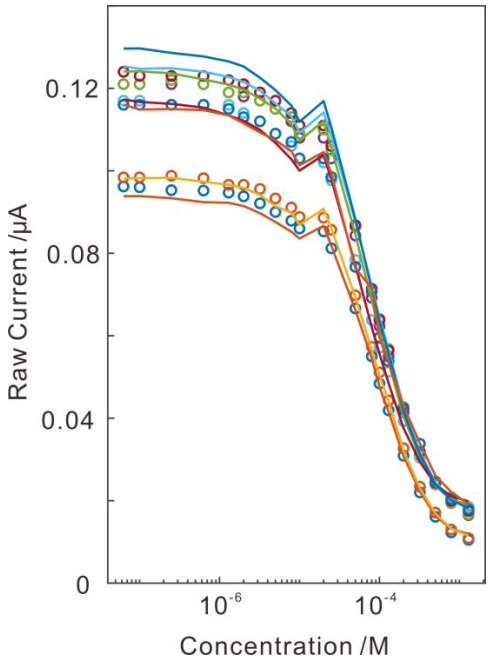

Figure S4. Global fitting of the outputs of kanamycin-detecting sensors in PBS. We globally fit the output of a training set of seven kanamycin-detecting sensors to Eq. 2 to define K_D, α, and γ for this type of sensor under these conditions. The solid lines illustrate how well the globally fit parameters describe the output of each individual sensor.

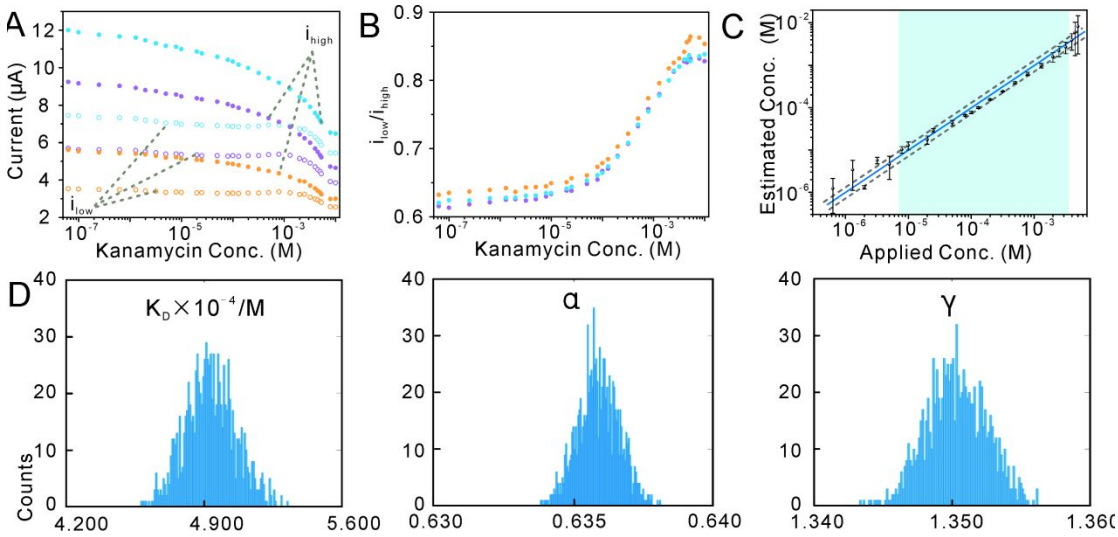

Figure S5. The kanamycin-detecting sensors test in whole blood without calibration. (A) The sensors exhibited significant variations for currents at high (i_{high}) or low potentials (i_{low}). (B) The ratio of i_{low} to i_{high} is quite reproducible for different sensors. (C) Finally, we recover kanamycin concentration estimates over a 405-fold concentration range from 7.9×10^{-6} M to 3.2×10^{-3} M in whole blood. (D) Optimized parameters obtained via global fitting. The squared errors in the fittings (Figure S6) were propagated by Monte-Carlo analysis in order to provide a distribution of the variability in the calculated parameters K_D, α, and γ.

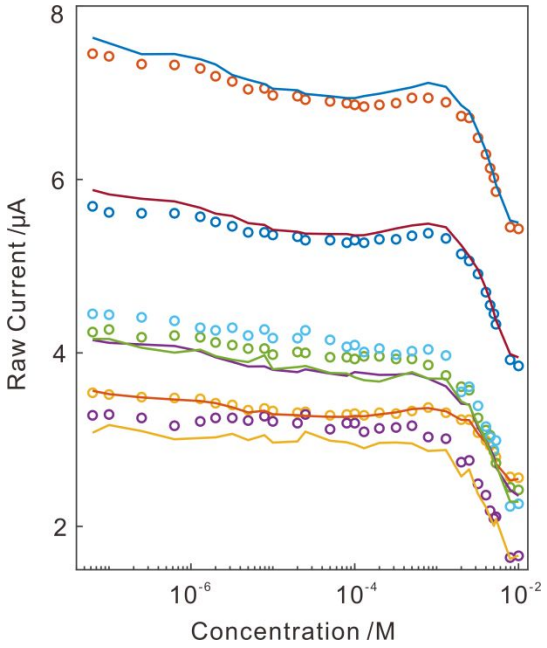

Figure S6. Global fitting of the outputs of kanamycin-detecting sensors in whole blood. We globally fit the output of a training set of six kanamycin-detecting sensors to Eq. 2 to define K_D, α, and γ for this type of sensor under these conditions.

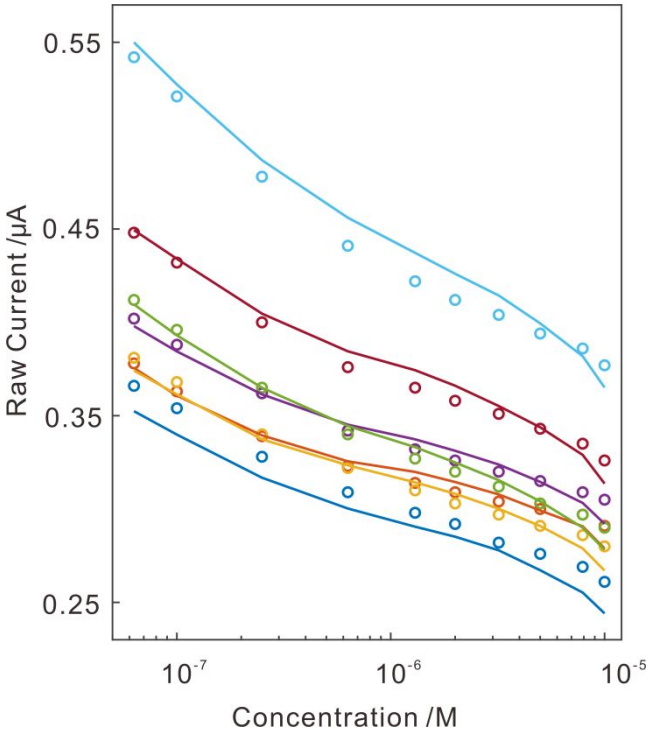

Figure S7. Global fitting of the outputs of doxorubicin-detecting sensors in PBS. We globally fit the output of a training set of seven doxorubicin-detecting sensors to Eq. 2 to define K_D, α, and γ for this type of sensor under these conditions.

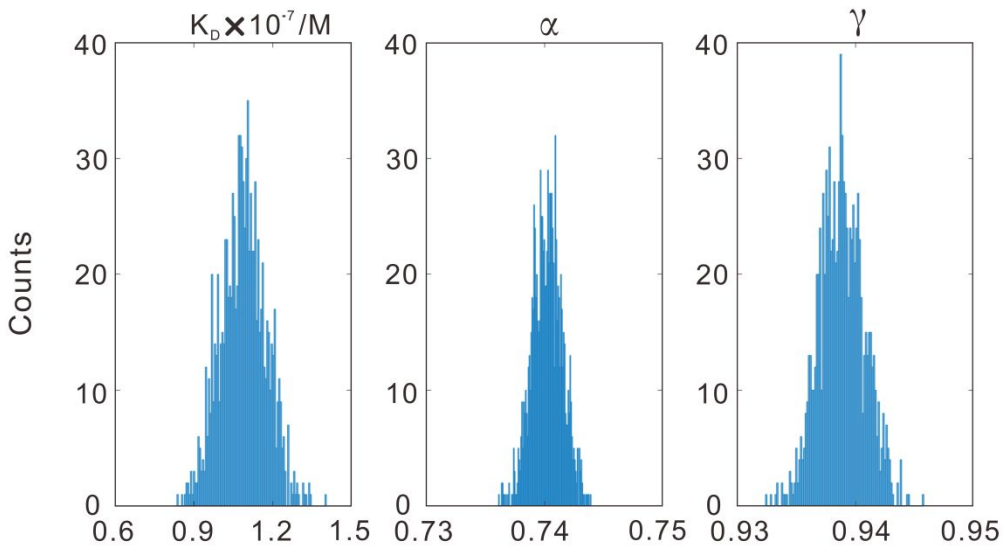

Figure S8. Optimized parameters obtained via global fitting. The squared errors in the fittings (Figure S7) were propagated by Monte-Carlo analysis in order to provide a distribution of the variability in the calculated parameters K_D, α, and γ.

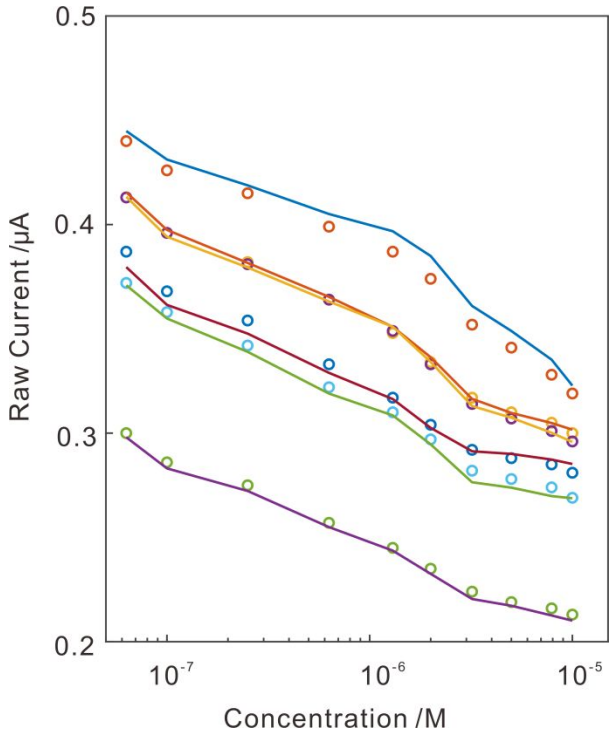

Figure S9. Global fitting of the outputs of doxorubicin-detecting sensors in whole blood. We globally fit the output of a training set of six doxorubicin-detecting sensors to Eq. 2 to define K_D, α, and γ for this type of sensor under these conditions.

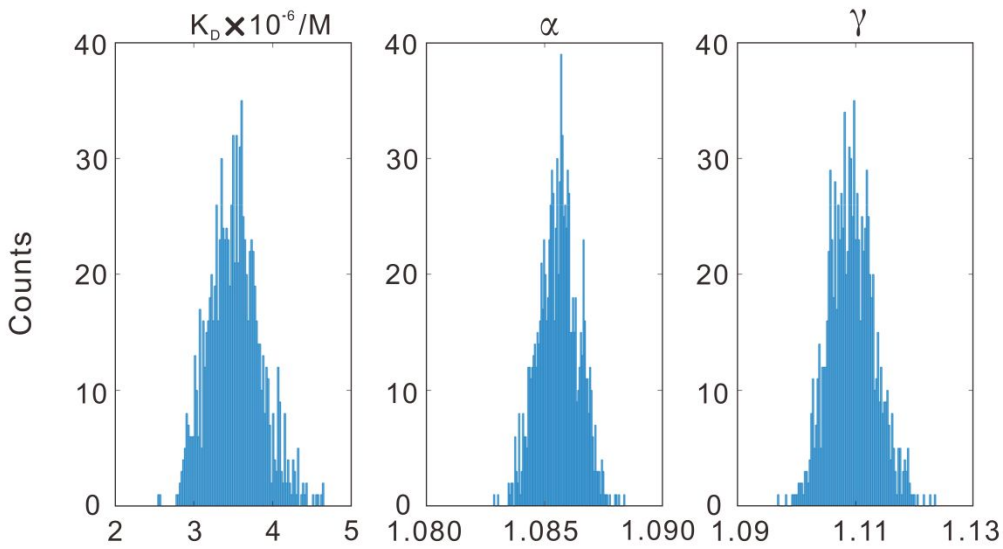

Figure S10. Optimized parameters obtained via global fitting. The squared errors in the fittings (Figure S9) were propagated by Monte-Carlo analysis in order to provide a distribution of the variability in the calculated parameters K_D, α, and γ.

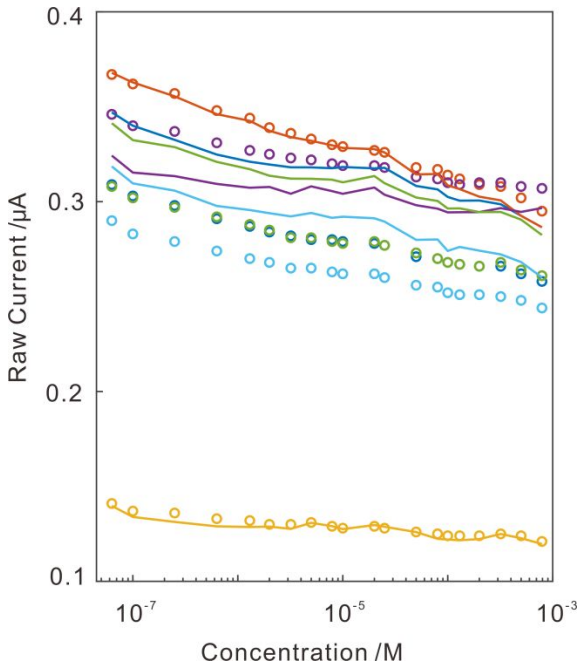

Figure S11. Global fitting of the outputs of ATP-detecting sensors in PBS. We globally fit the output of a training set of six ATP-detecting sensors to Eq. 2 to define K_D, α, and γ for this type of sensor under these conditions.

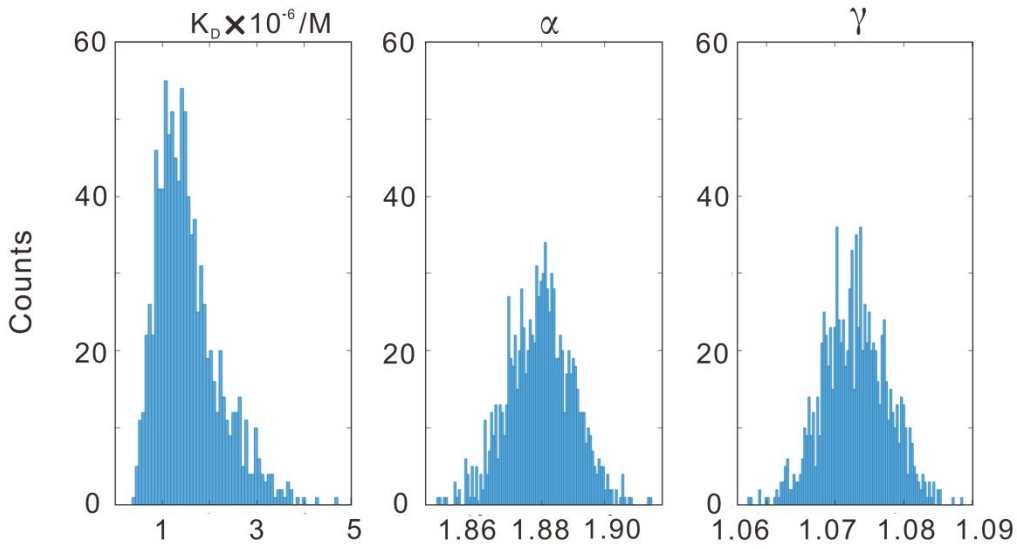

Figure S12. Optimized parameters obtained via global fitting. The squared errors in the fittings (Figure S11) were propagated by Monte-Carlo analysis in order to provide a distribution of the variability in the calculated parameters K_D, α, and γ.

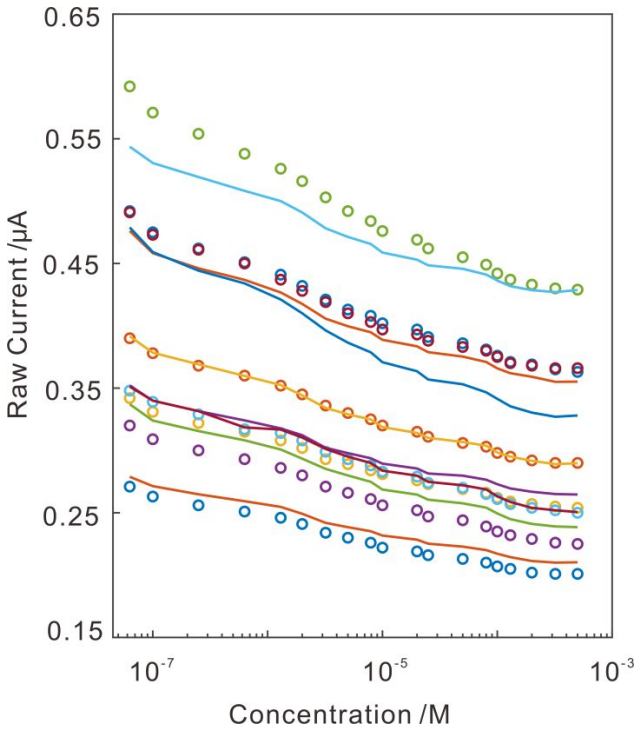

Figure S13. Global fitting of the outputs of ATP-detecting sensors in whole blood. We globally fit the output of a training set of eight ATP-detecting sensors to Eq. 2 to define K_D, α, and γ for this type of sensor under these conditions.

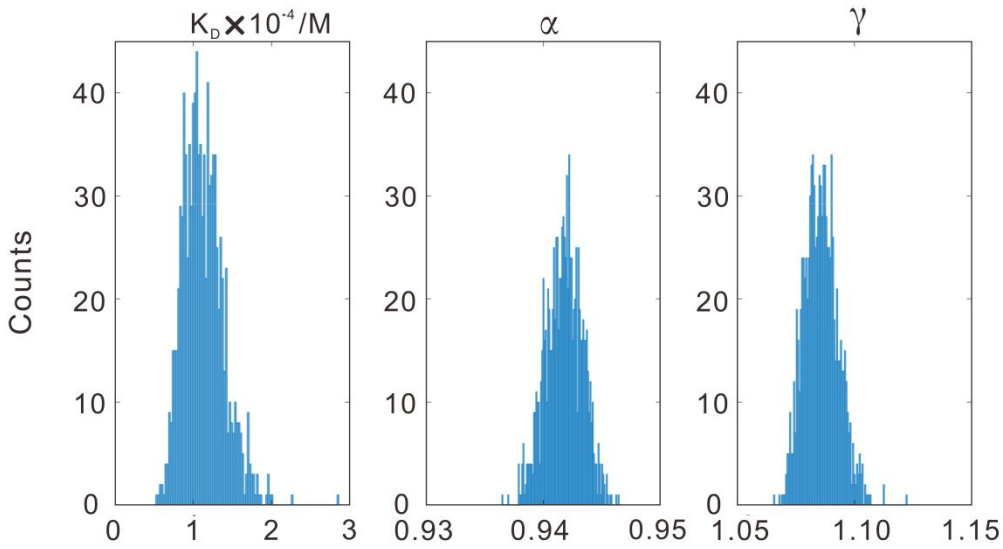

Figure S14. Optimized parameters obtained via global fitting. The squared errors in the fittings (Figure S13) were propagated by Monte-Carlo analysis in order to provide a distribution of the variability in the calculated parameters K_D, α, and γ.

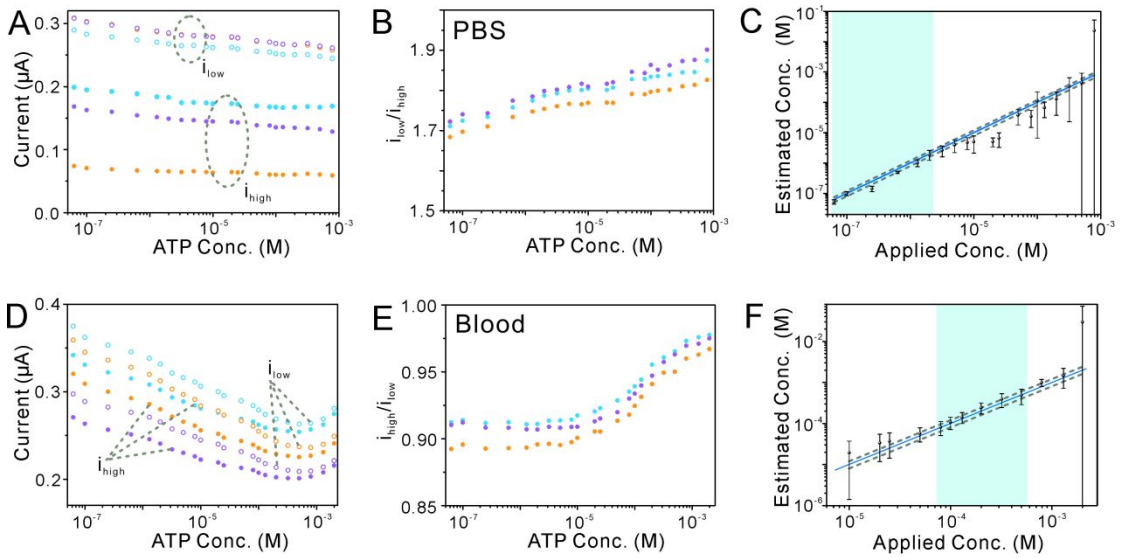

Figure S15. The ATP-detecting sensors test in PBS and whole blood without calibration. (A) A set of single-reporter, ATP-detecting sensors was challenged in PBS. It was clearly observed the i_{low} and the i_{high} vary dramatically in different sensors. (B) Conversely, the i_{low}/i_{high} was quite reproducible. (C) Specifically, this single-reporter, dual-peak, calibration-free approach produces ATP concentration in PBS estimates the actual concentration across from 6.3×10^{-8} M to 2.0×10^{-6} M, achieving an approximate 31.7-fold concentration range. (D) We prepared a new set of ATP-detecting sensors and challenged in whole blood. As expected, the i_{low} and the i_{high} vary dramatically in different sensors. (E) Conversely, the i_{high}/i_{low} was quite reproducible. (F) Specifically, this calibration-free approach produces ATP concentration in whole blood estimates the actual concentration across from 8.0×10^{-5} M to 5.0×10^{-4} M, achieving an approximate 6.25-fold concentration range. The dashed lines in panel C and F represent ±20% accuracy bands.

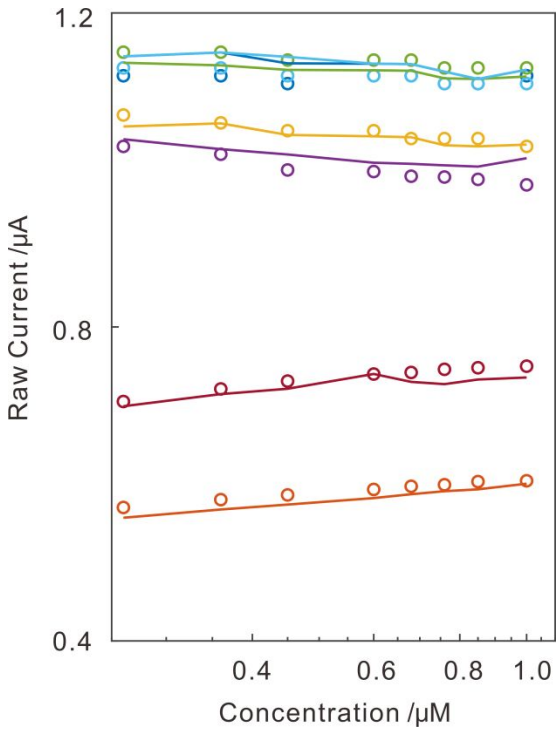

Figure S16. Global fitting of the outputs of thrombin-detecting sensors in tris buffer. We globally fit the output of a training set of seven thrombin-detecting sensors to Eq. 2 to define K_D, α, and γ for this type of sensor under these conditions.

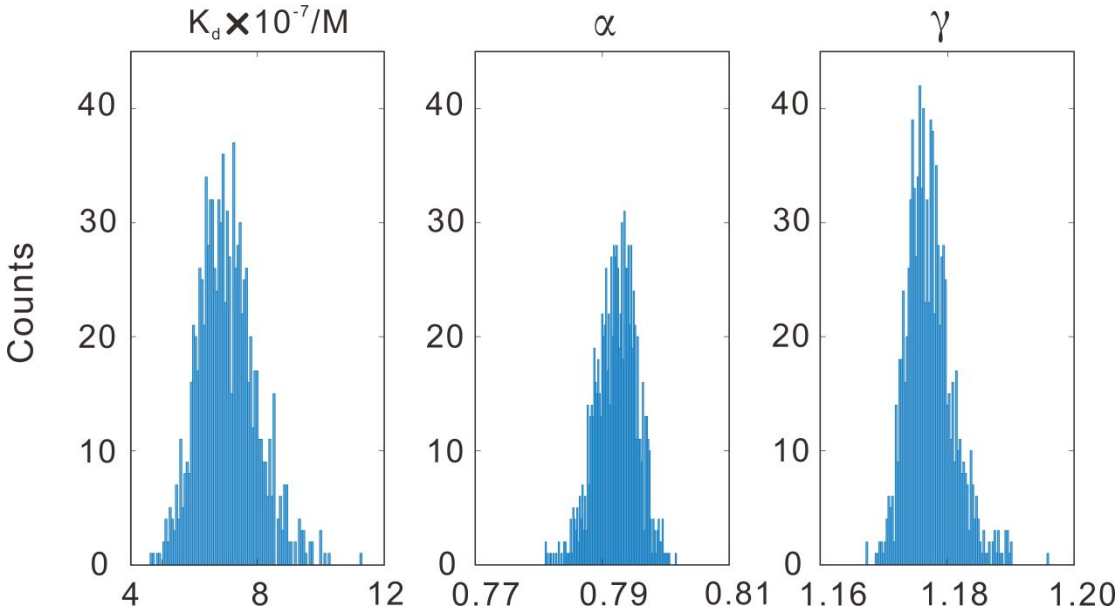

Figure S17. Optimized parameters obtained via global fitting. The squared errors in the fittings (Figure S16) were propagated by Monte-Carlo analysis in order to provide a distribution of the variability in the calculated parameters K_D, α, and γ.

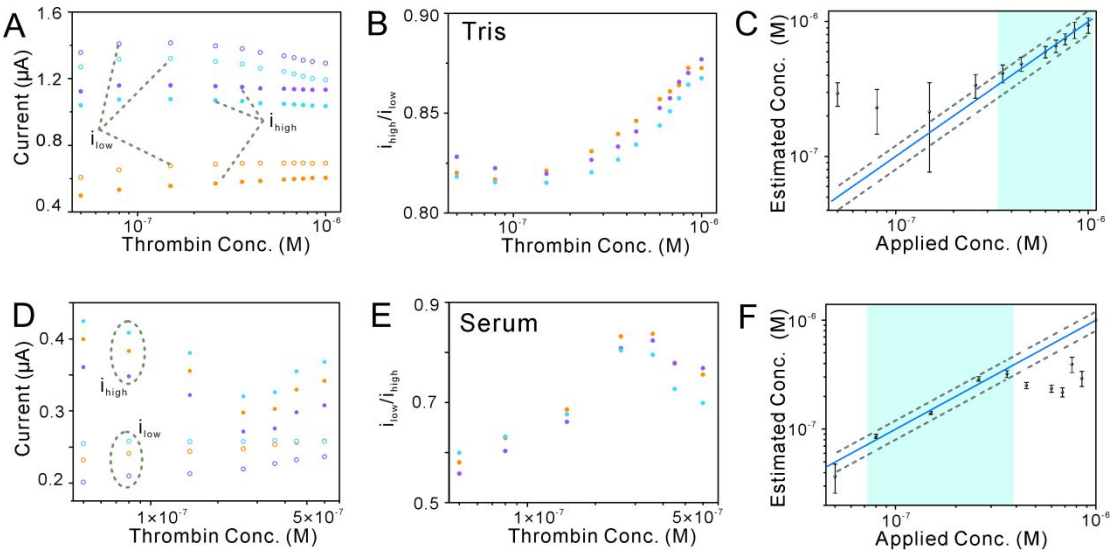

Figure S18. The thrombin-detecting sensors test in tris buffer and diluted serum without calibration. (A) A set of single-reporter, thrombin-detecting sensors was challenged in tris buffer. It was clearly observed that the i_{low} and the i_{high} vary dramatically in different sensors. (B) Conversely, the i_{high}/i_{low} was quite reproducible. (C) Specifically, this single-reporter, dual-peak, calibration-free approach produces thrombin concentration in whole blood estimates the actual concentration across from 3.6×10^{-7} M to 1.0×10^{-6} M, achieving an approximate 2.8-fold concentration range. (D) We prepared a new set of thrombin-detecting sensors and challenged in diluted serum. As expected, the i_{low} and the i_{high} vary dramatically in different sensors. (E) Conversely, the i_{low}/i_{high} was quite reproducible. (F) Specifically, this calibration-free approach produces thrombin concentration in diluted serum estimates the actual concentration across from 8.0×10^{-8} M to 3.6×10^{-7} M, achieving an approximate 4.5-fold concentration range. The dashed lines in panel C and F represent ±20% accuracy bands.

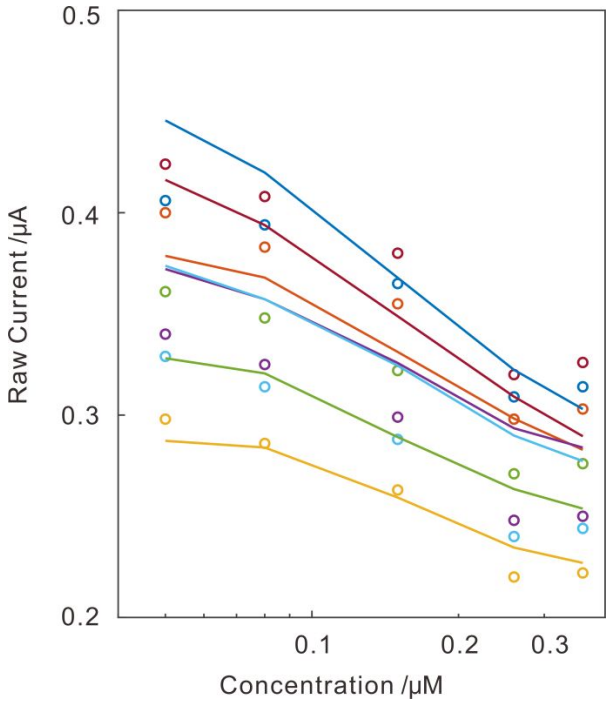

Figure S19. Global fitting of the outputs of thrombin-detecting sensors in diluted serum. We globally fit the output of a training set of seven thrombin-detecting sensors to Eq. 2 to define K_D, α, and γ for this type of sensor under these conditions.

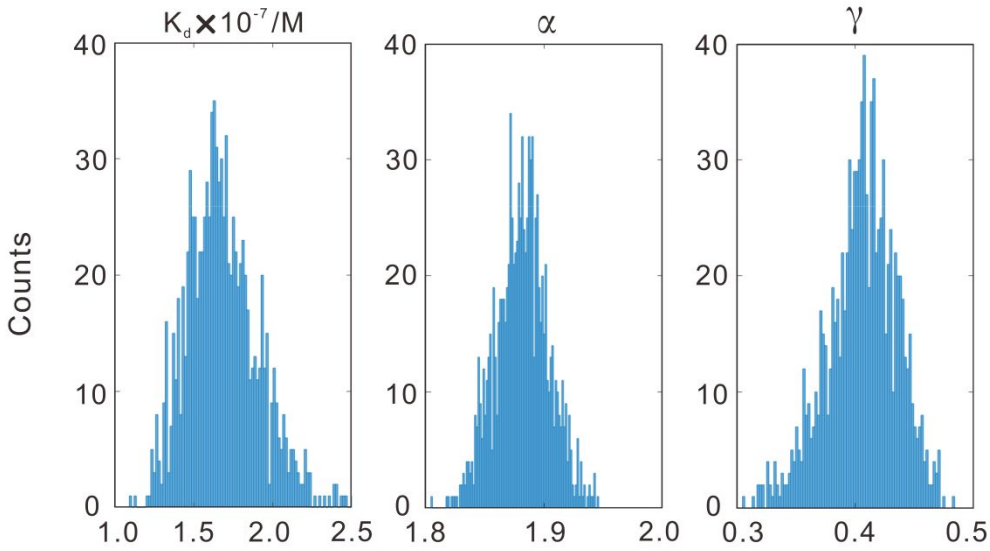

Figure S20. Optimized parameters obtained via global fitting. The squared errors in the fittings (Figure S19) were propagated by Monte-Carlo analysis in order to provide a distribution of the variability in the calculated parameters K_D, α, and γ.

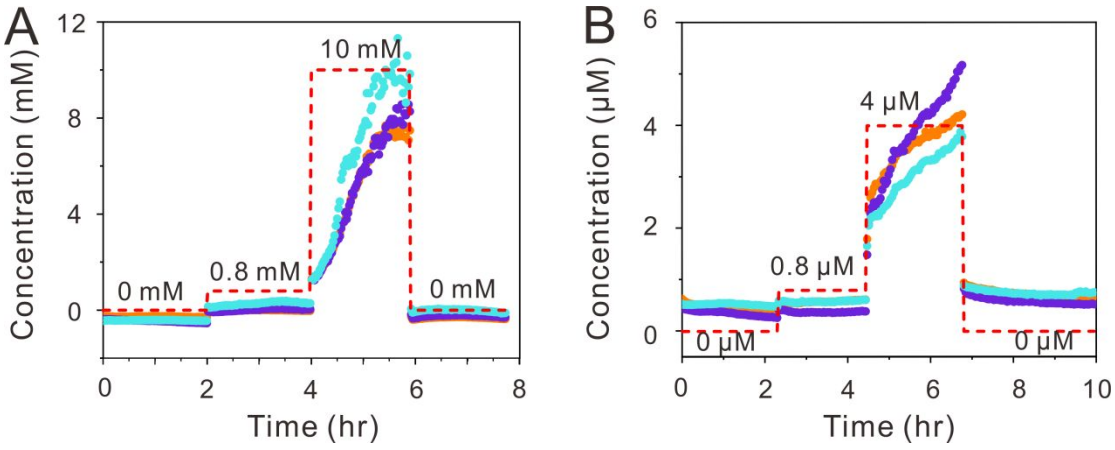

Figure S21. Calibration-free measurement of kanamycin (A) and doxorubicin (B) test in vitro. Even under these demanding conditions, the dual-peak calibration-free sensors are reproducible and the baselines (0.0 mM target) of the sensors are well recovered after all kanamycin have been cleaned, and the measured concentration of the sensor is relatively consistent with the actual concentration.

Table S1. The parameters determined by fitting titration data in buffer solution obtained from the"dual-peak" strategy sensors via a Hill equation.

target	sample	Parameters		
		α	K_D (μM)	γ
kanamycin	PBS	0.61698	51.087	1.407158
ATP	PBS	1.89034	1.443	1.074999
doxorubicin	PBS	0.74021	0.011	0.938833
thrombin	tris	0.79237	0.697	1.176515

Table S2. The parameters determined by fitting titration data in complex

solution obtained from the“dual-peak” strategy sensors via a Hill equation.

target	sample	Parameters		
		α	K_D (mM)	γ
kanamycin	blood	0.63617	0.497372	1.351213
ATP	blood	0.93896	0.108577	1.087198
doxorubicin	blood	1.08555	0.003501	1.109631
thrombin	serum	1.89103	0.000170	0.398332

Table S3 Single and dual peak distribution table of single reporter in kanamycin-detecting sensors under different test parameters in PBS.

kanamycin test in PBS											
Freq Amp	2	5	10	15	20	30	50	60	120	200	500
50	single	dual	dual	dual	single	single	single	single	single	single	single
75		dual	dual	dual	dual	dual	single	single	single	single	single
100		dual	dual	dual	dual	dual	dual	dual	dual	single	single
125		dual	dual	dual	dual	dual	dual	dual	dual	dual	single
150		dual	dual	dual	dual	dual	dual	dual	dual	dual	single
175		dual	dual	dual	dual	dual	dual	dual	dual	dual	single
200		dual	dual	dual	dual	dual	dual	dual	dual	dual	single

Table S4 Single and dual peak distribution table of single reporter in kanamycin-detecting sensors under different test parameters in blood.

kanamycin test in blood

Freq Amp	2	5	10	15	20	30	50	60	120	200	500
50	single	dual	dual	single	single	single	single	single	single	single	single
75	dual	dual	dual	dual	dual	dual	single	single	single	single	single
100	dual	dual	dual	dual	dual	dual	dual	dual	single	single	single
125		dual	dual	dual	dual	dual	dual	dual	single	single	single
150		dual	dual	dual	dual	dual	dual	dual	dual	single	single
175		dual	dual	dual	dual	dual	dual	dual	dual	single	single
200			dual	dual	dual	dual	dual	dual	dual	dual	single

Table S5 Single and dual peak distribution table of single reporter in ATP-detecting sensors under different test parameters in PBS.

ATP test in PBS											
Freq Amp	2	5	10	15	20	30	50	60	120	200	500
50	single	single	single	single	single	single	single	single	single	single	single
75	single	single	dual	dual	dual	single	single	single	single	single	single
100	single	single	dual	dual	dual	dual	dual	single	single	single	single
125	dual	dual	dual	dual	dual	dual	dual	dual	dual	single	single
150	dual	dual	dual	dual	dual	dual	dual	dual	dual	single	single
175	dual	dual	dual	dual	dual	dual	dual	dual	dual	single	single
200		dual	dual	dual	dual	dual	dual	dual	dual	single	single

Table S6 Single and dual peak distribution table of single reporter in ATP-detecting sensors under different test parameters in blood.

ATP test in blood											
Freq Amp	2	5	10	15	20	30	50	60	120	200	500
50	single	single	single	single	single	single	single	single	single	single	single
75	single	single	dual	dual	dual	dual	single	single	single	single	single
100	single	dual	dual	dual	dual	dual	single	single	single	single	single
125	dual	dual	dual	dual	dual	dual	dual	single	single	single	single
150	dual	dual	dual	dual	dual	dual	dual	dual	single	single	single
175	dual	dual	dual	dual	dual	dual	dual	dual	dual	single	single
200		dual	dual	dual	dual	dual	dual	dual	dual	single	single

Table S7 Single and dual peak distribution table of single reporter in doxorubicin -detecting sensors under different test parameters in PBS.

doxorubicin test in PBS											
Freq Amp	2	5	10	15	20	30	50	60	120	200	500
50	single	single	single	single	single	single	single	single	single	single	single
75	single	single	dual	dual	dual	dual	single	single	single	single	single
100	single	single	dual	dual	dual	dual	dual	dual	single	single	single
125	dual	dual	dual	dual	dual	dual	dual	dual	dual	single	single
150	dual	dual	dual	dual	dual	dual	dual	dual	dual	single	single
175	dual	dual	dual	dual	dual	dual	dual	dual	dual	single	single
200			dual	dual	dual	dual	dual	dual	dual	dual	dual

Table S8 Single and dual peak distribution table of single reporter in

doxorubicin -detecting sensors under different test parameters in blood.

doxorubicin test in blood											
Freq Amp	2	5	10	15	20	30	50	60	120	200	500
50	single	single	dual	dual	single	single	single	single	single	single	single
75	single	single	dual	dual	dual	dual	single	single	single	single	single
100	single	dual	dual	dual	dual	dual	dual	dual	single	single	single
125	dual	dual	dual	dual	dual	dual	dual	dual	dual	single	single
150	dual	dual	dual	dual	dual	dual	dual	dual	dual	single	single
175			dual	dual	dual	dual	dual	dual	dual	single	single
200			dual	dual	dual	dual	dual	dual	dual	dual	dual

Table S9 Single and dual peak distribution table of single reporter in thrombin -detecting sensors under different test parameters in tris buffer.

thrombin test in tris buffer										
Freq Amp	2	5	10	15	20	30	60	120	200	500
50	single	single	dual	dual	single	single	single	single	single	single
75		dual	dual	dual	single	single	single	single	single	single
100		dual	dual	dual	single	single	single	single	single	single
125		dual	dual	dual	dual	dual	single	single	single	single
150		dual	dual	dual	dual	dual	dual	single	single	single
175				dual	dual	dual	dual	single	single	single
200			dual	dual	dual	dual	dual	dual	single	single

Table S10 Single and dual peak distribution table of single reporter in thrombin-detecting sensors under different test parameters in diluted serum.

thrombin test in serum										
Freq Amp	2	5	10	15	20	30	60	120	200	500
50	single	single	single	single	single	single	single	single	single	single
75	dual	dual	single	single	single	single	single	single	single	single
100	dual	dual	dual	dual	single	single	single	single	single	single
125	dual	dual	dual	dual	dual	single	single	single	single	single
150	dual	dual	dual	dual	dual	dual	single	single	single	single
175	dual	dual	dual	dual	dual	dual	dual	single	single	single
200		dual	dual	dual	dual	dual	dual	single	single	single

Table S11 SWV test parameters used for different sensors in this work.

Target	Sample	Parameters	
		Amp /mV	Freq /Hz
kanamycin	PBS	50	15
	Blood	150	120
ATP	PBS	100	15
	Blood	75	10
doxorubicin	PBS	50	10
	Blood	50	12
thrombin	Tris	125	10
	serum	150	5